Demystifying the role of surfactant in tailoring polyamide morphology for enhanced RO performance: Mechanistic insights and environmental implications

Qimao Gan,[†] Lu Elfa Peng,[*,†] Zhe Yang,[†] Peng-Fei Sun,[†] Li Wang,[†] Hao Guo,[†] Chuyang Y. Tang[*,†]

[†]Department of Civil Engineering, The University of Hong Kong, Pokfulam, Hong Kong SAR 999077, P. R., China.

[*]Corresponding Authors:

Lu Elfa Peng, Email: elfapeng@connect.hku.hk, Phone: +852-53964327

Chuyang Y. Tang, Email: tangc@hku.hk, Phone: +852-28591976

22 **TABLE OF CONTENT**

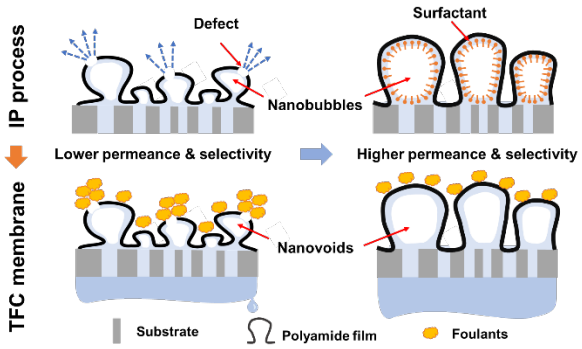

23

24

ABSTRACT

Surfactant-assisted interfacial polymerization (IP) has shown strong potential to improve the separation performance of thin film composite polyamide membranes. A common belief is that the enhanced performance is attributed to accelerated amine diffusion induced by surfactant, which promotes the IP reaction. However, we show enhanced membrane performance for Tween 80 (a common surfactant) even though it decreased the amine diffusion. Indeed, the membrane performance is closely related to its polyamide roughness features with numerous nanovoids. Inspired by the nanofoaming theory that relates the roughness features to nanobubbles degassed during the IP reaction, we hypothesize that the surfactant can stabilize the generated nanobubbles to tailor the formation of nanovoids. Accordingly, we obtained enlarged nanovoids when the surfactant was added below its critical micelle concentration (CMC). In addition, both the membrane permeance and selectivity were enhanced thanks to the enlarged nanovoids and reduced defects in the polyamide layer. Increasing the concentration above CMC resulted in shrunken nanovoids and deteriorated performance, which can be ascribed to the decreased stabilization effect caused by micelle formation. Interestingly, better anti-fouling performance was also observed for the surfactant-assisted membranes. Our current study provides mechanistic insights into the critical role of surfactant during the IP reaction, which may have important implications for more efficient membrane-based desalination and water reuse.

KEYWORDS: *reverse osmosis (RO) membranes, polyamide nanovoids, surfactant, stabilization effect, defects, membrane fouling*

SYNOPSIS

Surfactant-assisted interfacial polymerization promotes larger nanovoids and minimize defects in polyamide layer due to the stabilization effect, achieving enhanced membrane separation performance and anti-fouling ability.

INTRODUCTION

Thin film composite (TFC) reverse osmosis (RO) membranes have been widely applied for desalination and water reuse,[1-4] largely attributed to the excellent separation property of their polyamide rejection layers.[5-10] These polyamide layers are typically fabricated on porous substrates by interfacial polymerization (IP) of amine (e.g., *m*-phenylenediamine, MPD) in water and trimesoyl chloride (TMC) in hexane. Extensive research efforts have been devoted to regulating the IP reaction to enhance membrane performance, such as applying additives into the two phases.[11-13] Surfactant, as a common additive, has been widely reported to significantly improve membrane permeance and selectivity,[11, 12, 14-21] which attracts increasing research interests in deciphering the underlying mechanisms.

A common belief is that the enhanced membrane permeance and/or selectivity by surfactants is ascribed to the improved amine diffusion into the organic phase, which can promote the IP reaction.[14, 16-21] Specifically, some studies reported that the facilitated diffusion could be explained by the reduced interfacial tension or increased wetting of the substrate by surfactants.[16-18, 21] Several researchers attributed the accelerated diffusion to the opposite charge properties between the amine monomers and surfactants.[19, 20] Nevertheless, our preliminary experimental results show that although three common surfactants (sodium dodecyl sulfate (SDS), Tween 80 (TW), and cetyltrimethylammonium bromide (CTAB)) improved the membrane permeance and selectivity, SDS increased amine diffusion while TW and CTAB decreased the diffusion. This peculiar phenomenon prompts us to further investigate the exact mechanism(s) on how surfactants regulate membrane performance. Indeed, the membrane performance has been widely reported to be dependent on the nanovoids-containing roughness feature of its polyamide layer.[5, 6, 12, 22-26] Specifically, more

prominent nanovoids could typically lead to higher membrane permeance thanks to the increased filtration area[26-28] and gutter effect.[27, 29-31] Presumably, surfactants may benefit the formation of nanovoids during the IP reaction to promote membrane performance.

Herein, we provide an alternative interpretation on the role of surfactants. A recent nanofoaming theory by Tang and co-workers[26, 27, 32-37] revealed that the nanovoids of polyamide layer were formed by the interfacial degassing/vaporization. In this theory, gas/vapor nanobubbles would be generated due to the H^+ and heat released from the IP reaction. These nanobubbles could be further confined between the polyamide layer and the substrate, leading to the formation of nanovoids-containing roughness feature (**Figure 1a**). However, some nanobubbles may dissolve again or burst due to high internal Laplace pressure[38-41] or escape through the substrate pores[34, 36], which can suppress the formation of nanovoids. Interestingly, surfactants are commonly used to increase the stability of bubbles[42, 43] and have been reported to effectively stabilize nanobubbles at a liquid-solid interface[44-46]. Therefore, we hypothesize that surfactants can stabilize the generated nanobubbles at the IP reaction interface. This stabilization effect of surfactants can contribute to forming more prominent nanovoids in the polyamide layer toward enhanced membrane performance (**Figure 1b**).

To verify the hypothesis, we investigated the role of surfactant, particularly its concentration, in tailoring the polyamide nanovoids and membrane permeance. In addition, we further revealed the improved salt rejection and reduced fouling propensity for the surfactant-assisted RO membranes. Our current study provides new mechanistic insights into the role of surfactant during the IP reaction, which may have important implications for more efficient membrane-based desalination and water reuse.

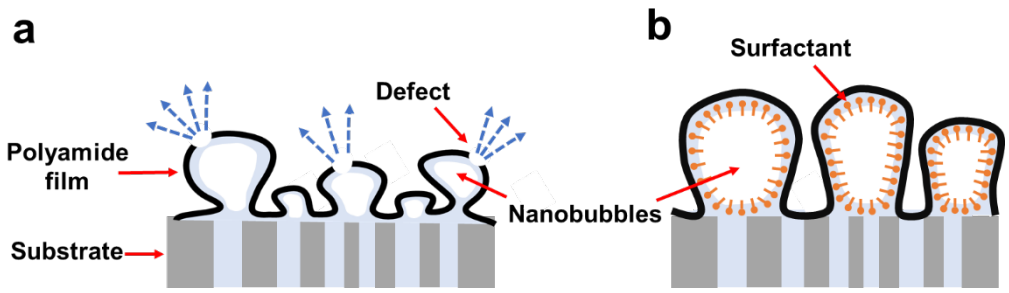

Figure 1. Schematic diagrams of polyamide nanovoids formation under: (a) conventional IP process and (b) surfactant-assisted IP process. See more details in **Supporting Information S3**.

MATERIALS AND METHODS

Chemicals. *m*-phenylenediamine (MPD, 99%, Sigma-Aldrich), trimesoyl chloride (TMC, 98%, Sigma-Aldrich), *n*-hexane (Sigma-Aldrich), and commercial polysulfone (PSf) substrates (MWCO 67 kDa, Vontron Technology) were used to prepare polyamide RO membranes through IP process. To investigate the role of surfactant in membrane formation, three commonly used surfactants (**Figure 2**) were adopted: an anionic surfactant sodium dodecyl sulfate (SDS, $C_{12}H_{25}NaSO_4$, Mw ~ 288.4, Dieckmann), a cationic surfactant cetyltrimethylammonium bromide (CTAB, $C_{16}H_{33}N(CH_3)_3Br$, Mw ~ 364.5, Dieckmann), and a non-ionic surfactant Tween 80 (TW, $C_{64}H_{124}O_{26}$, Mw ~ 1310, Dieckmann). Non-ionic TW was further selected as the model surfactant to better resolve the effect of the stabilization effect from other potential competing effects (e.g., changed MPD diffusion rate due to charge interaction). Sodium chloride (NaCl, Dieckmann) and humic acid (HA, Sigma-Aldrich) were used for membrane performance tests.

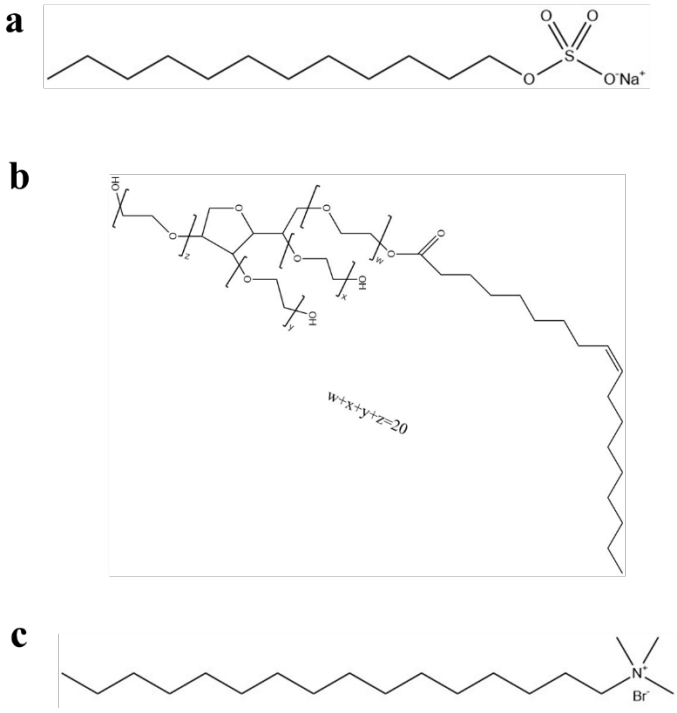

Figure 2. Chemical structures of (a) SDS, (b) TW and (c) CTAB.

MPD diffusion into the organic phase. The MPD diffusion was measured by recording the diffused MPD from the aqueous phase into the organic phase using an ultraviolet–visible spectrophotometer (UV/VIS, UH5300, Hitachi).[47] Briefly, 0.3 ml of MPD solution with/without surfactant was added into the bottom of a quartz cuvette (~3 ml capacity) with the height of the solution below the optical path of the spectrophotometer. 2.7 mL of hexane was then gently added on top of the MPD solution. The diffused MPD in the hexane phase, which is proportional to the absorbance intensity, was recorded for 1 min (consistent with the IP reaction time) by the spectrophotometer at the wavelength of 294 nm.

Preparation of TFC polyamide membranes. Conventional TFC membranes were prepared by performing IP reaction between MPD (0.2-8 w/w%, dissolved in water) with/without surfactant and TMC (0.1 w/w%, dissolved in hexane) on the PSf substrates. Briefly, the MPD solution with/without surfactant was firstly used to immerse the substrate for 2 min. After using a rubber roller to remove the excess MPD solution, the TMC solution was then applied to immerse the substrate for 1 min to form the polyamide film. Lastly, the resulting polyamide membrane was rinsed by hexane and post-treated in 50 °C water for 10 min. The prepared TFC membranes were named as TFC-MPD concentration surfactant concentration, e.g., TFC-0.5TW0.001 for the one prepared using 0.5 w/w% MPD with 0.001 w/w% TW.

Preparation of free-interface polyamide membranes. To further resolve the role of surfactant, we prepared polyamide membranes through a free interface IP process.[34, 37, 48-51] Briefly, a MPD solution (0.5 and 2 w/w%) with/without TW and a 0.1 w/w% TMC/hexane solution were allowed to react for 1 min at a substrate-free interface. The resulting polyamide layer was then loaded onto the PSf substrate under the assistance of vacuum filtration.

Characterizations of polyamide membranes. The top side structures of polyamide membranes were characterized by Field-emission scanning electron microscopy (FE-SEM, S-4800, Hitachi) at an accelerating voltage of 5.0 kV. All samples were dried, and sputter coated with a thin layer of gold before SEM characterization. The cross-sectional structures of the membranes were resolved by Transmission electron microscopy (TEM, CM100, Philips) at an accelerating voltage of 100 kV. The elemental composition of membrane surface was analyzed by X-ray photoelectron spectroscopy (XPS, Thermo Fishier Scientific) using an X-ray source of Al Kα gun with a spectra range of 0−1350 eV.

Membrane separation performance. Water flux and NaCl rejection of the membranes were tested using a laboratory-scale crossflow RO filtration setup.[35] Each membrane coupon (a filtration area of 42.0 cm^2) was pre-compacted at 17.0 bar for 1.5 h. The test was then performed at 15.5 bar with a NaCl feed solution (2000 ppm) at a crossflow velocity of 22.4 cm/s under room temperature (~25 °C). The water flux J_v (L m^{-2} h^{-1}) and water permeance A (L m^{-2} h^{-1} bar^{-1}) were calculated by:

$$J_v = \frac{\Delta m}{\Delta t \times a \times \rho} \quad (1)$$

$$A = \frac{J_v}{\Delta P - \Delta \pi} \quad (2)$$

where Δm (kg) is the mass of permeate during a time interval of Δt (h), a (m^2) is the membrane filtration area, ρ (kg/m^3) is the density of water, ΔP (bar) and $\Delta \pi$ (bar) are the transmembrane pressure and the transmembrane osmotic pressure, respectively. NaCl rejection (R) and NaCl permeability coefficient (B) was calculated by:[11, 52, 53]

$$R = \frac{C_f - C_p}{C_f} \times 100\% \quad (3)$$

$$B = (\frac{1}{R} - 1) \times J_v \quad (4)$$

where C_f and C_p are NaCl concentrations in the feed and the permeate, respectively, which were obtained based on conductivity measurements (Ultrameter II, Myron L). The water-NaCl perm-selectivity was represented by the *A/B* ratio.[11, 53]

Similarly, HA rejection was tested using a 100 ppm HA feed solution (pH at ~6.5) and was also calculated by Equation (3). The concentrations of HA in the feed and the permeate were measured by a total organic carbon (TOC) analyzer (TOC-L CPH, SHIMADZU).

Membrane fouling tests. A membrane sample with a filtration area of 12 cm^2 was pre-compacted with a 2000 ppm NaCl feed solution at 17.0 bar for 12 h with a crossflow velocity of 11.2 cm/s at room temperature (~25 °C). To conduct the fouling test, the initial flux was adjusted to 17 L m^{-2} h^{-1} and 100 ppm HA was introduced to the feed solution (the resultant pH was at ~6.5). Each fouling test was continued for 96 h. Fouled membranes were immersed in 50 mL of 0.1 M sodium hydroxide in separate tubes. These tubes were then shaken on an orbital shaker overnight to extract the deposited HA on the membranes since HA can be easily dissolved at pH > 12.[54, 55] Similar extraction method was also reported in other studies.[47, 56-58] The HA concentration was determined by an ultraviolet–visible spectrophotometer (UV/VIS, UH5300, Hitachi) at the wavelength of 254 nm.[47, 58]

RESULTS AND DISCUSSION

Effects of different surfactants on MPD diffusion and membrane performance. Researchers commonly believe that surfactant addition can improve the amine diffusion in the organic phase, thus promoting the IP reaction for enhanced membrane performance.[14, 16-21] This seems to be consistent with the increased MPD diffusion (**Figure 3a**) and enhanced permeance (**Figure 3b**) as well as selectivity (**Figure 3c**) by SDS in the current study. However, the addition of TW or CTAB could also improve the membrane separation performance (**Figure 3b** and **c**) despite their significantly decreased MPD diffusion (**Figure 3a**). The contradictory results between SDS, TW, and CTAB were also observed at higher MPD concentration of 2 w/w% (**Figure S1**), which indicated that the MPD diffusion alone is not sufficient to explain the role of surfactants. We further found that all surfactants could enlarge the polyamide nanovoids (**Figure S2**), which corresponded well with the enhanced membrane permeance. These observations could be explained by our hypothesis that surfactants can mitigate the dissolution/escape of nanobubbles by stabilizing them at the IP reaction interface, leading to more prominent nanovoids and higher water permeance (**Figure 1b**). In the current study, all the three surfactants were able to significantly enhance water permeance, revealing that the stabilization effect may play a dominant role.

To further reveal the stabilization effect of surfactant, we prepared polyamide films at a substrate-free IP reaction interface with/without surfactant. According to the nanofoaming theory, the generated nanobubbles would escape from the free interface due to the lack of confinement effect of the substrate, leading to a smooth polyamide film.[34, 36, 37, 47] As expected, we observed relatively smooth polyamide surfaces in the absence of surfactant (**Figure S3**). In contrast, all surfactants investigated in the current study were able to result in rougher polyamide films with more nodules and/or leaf-like

structures (**Figure S3**), which may confirm that they can stabilize the generated nanobubbles at the IP reaction interface to mitigate their escape.

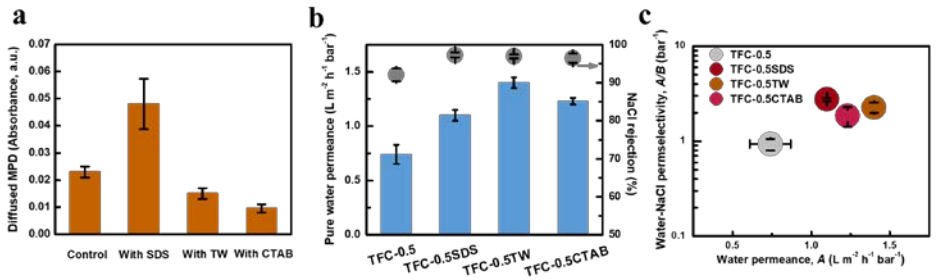

Figure 3. Effects of different surfactants (0.001 w/w% of SDS, TW, and CTAB, at MPD concentration of 0.5 w/w%) on (a) diffused MPD in the organic phase, (b) membrane separation performance, and (c) water-NaCl perm-selectivity.

Effects of TW concentration. To further investigate the stabilization effect of surfactant, a series of TW concentrations (CMC of ~0.00157 w/w%) were applied. Increased TW concentration resulted in monotonously decreased MPD diffusion (**Figure 4a**), which could be ascribed to the steric hindrance of TW at the water/hexane interface and thus reduced MPD diffusion.[20] Different from the trend of MPD diffusion, the water permeance of membranes firstly increased then declined as increasing TW concentration (**Figure 4b** and **c**), which corresponded well with their firstly enlarged then shrunken nanovoids (**Figure 5**). Specifically, the enlarged nanovoids and improved permeance of TFC-0.5TW0.001 and TFC-0.5TW0.0015 compared to TFC-0.5 can be attributed to the stabilization effect of TW. It is worth to note that TFC-0.5TW0.0015 gave relatively smaller nanovoids and lower water permeance than that of TFC-0.5TW0.001. In the current study, the addition of TW could result in two opposing effects: (1) reduced MPD diffusion (**Figure 4a**), which tends to suppress the formation of nanovoids due to less intensive IP reaction and (2) stabilization of nanobubbles, which tends to promote the formation of nanovoids. The final result depends on the competition of these two mechanisms. Further shrunken nanovoids and

decreased water permeance were observed for TFC-0.5TW0.003 despite its similar MPD diffusion to TFC-0.5TW0.0015 (**Figure 4a**). For TFC-0.5TW0.003, the corresponding TW concentration was above its CMC (~0.00157 w/w%). The formation of micelles under this condition can result in interfacial instabilities,[59, 60] leading to reduced stabilization effect of the surfactant during the IP reaction. Our results reveal the critical importance to optimize the dosage of surfactant.

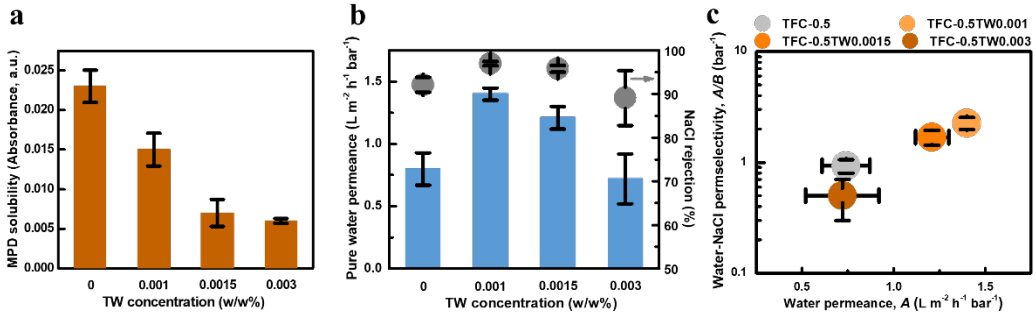

Figure 4. Effects of TW concentration (at MPD concentration of 0.5 w/w%) on (a) diffused MPD in the organic phase, (b) membrane separation performance, and (c) water-NaCl perm-selectivity.

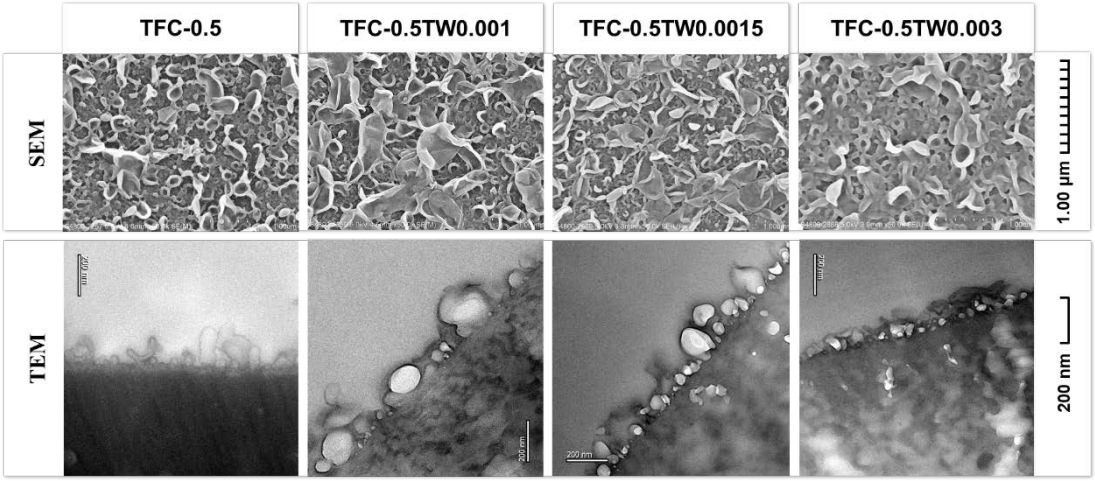

Figure 5. Effects of TW concentration on membrane surface structure (SEM top side view and TEM cross section view, at MPD concentration of 0.5 w/w%).

Effects of TW at different MPD concentrations. In order to further investigate the effects of TW on membrane performance and surface structure, different MPD concentrations were employed. Generally, increased MPD concentration resulted in promoted water permeance from TFC-0.2 to TFC-2 while declined permeance was

observed for TFC-8 (**Figure 6a**). This trend is consistent with previous studies.[27, 61, 62] The increased permeance can be attributed to the enlarged nanovoids from TFC-0.2 to TFC-2 (See the TEM graphs in **Figure 7**), which can be resulted from more generated nanobubbles by their higher MPD storage.[27] Previous studies have shown that nanovoids are effective in improving the water transport pathways in TFC membranes due to their "gutter effect".[27, 29-31] On the other hand, the declined permeance for TFC-8 can be explained by its thicker polyamide film (See the TEM graphs in **Figure 7**), which may offset the benefit of its larger nanovoids.[27] The addition of TW generally improved the water permeance compared to TFC membranes (**Figure 6a**) thanks to the more prominent nanovoids of TFC-TW membranes (**Figure 7**). Interestingly, the permeance enhancement by TW gradually decreased at higher MPD concentrations, e.g., the water permeance of TFC-2TW was only marginally higher than that of TFC-2 ($p = 0.10$). For the TFC membranes prepared at lower MPD concentrations (0.2 and 0.5 w/w%), the dissolution[38-41] and escape[34, 36] of the degassed nanobubbles could significantly suppress the formation of nanovoids when there were only a few nanobubbles generated due to the low MPD availability. For these membranes, the addition of TW could play a relatively more crucial role in forming larger nanovoids by mitigating the dissolution and escape of the inadequate nanobubbles. In contrast, for the TFC membranes prepared at higher MPD concentrations (2 and 8 w/w%), the stabilization effect of TW could be negligible when there are sufficient nanobubbles generated by high MPD availability. Indeed, the membranes without TW addition (TFC-2 and TFC-8) also show extensive presence roughness features (**Figure 7**).

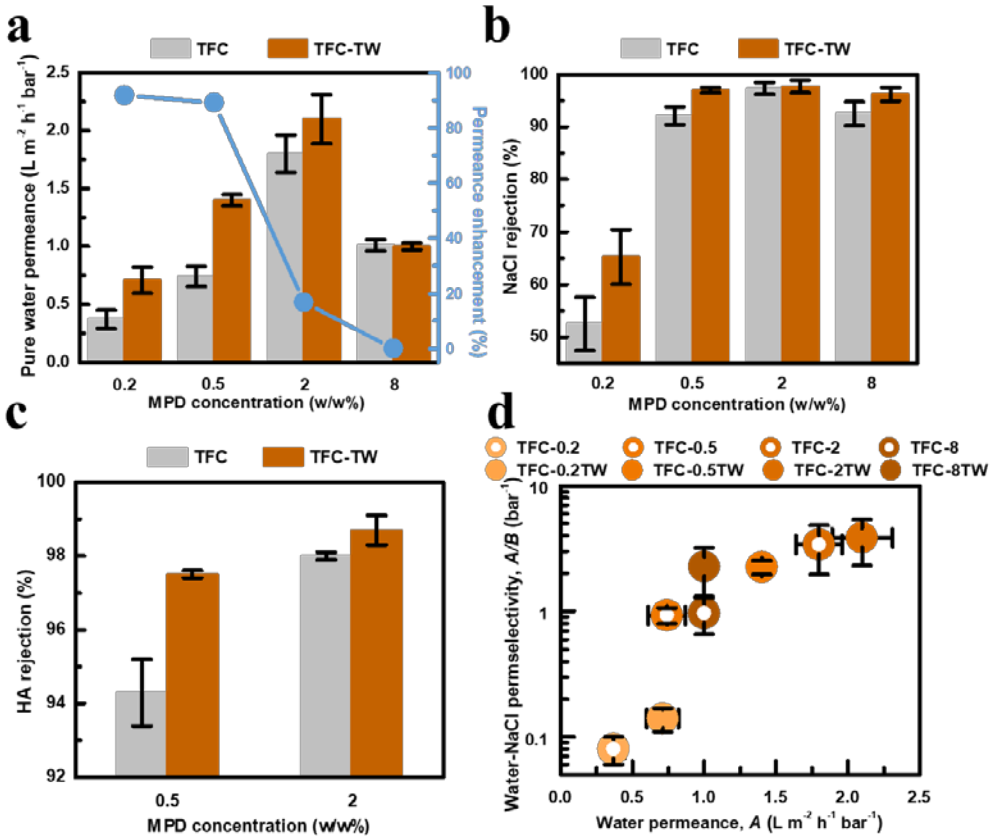

277

278 **Figure 6.** Effects of MPD concentration (at 0.001 w/w% TW) on (a) water permeance, (b) NaCl rejection,
279 (c) HA rejection, and (d) water-NaCl perm-selectivity.
280

281 Moreover, the addition of TW could generally improve the salt rejection of membranes
282 (**Figure 6b**) despite the similar PA cross-linking degree (indicated by the O/N ratio
283 from XPS measurements in **Figure S8a**) and surface charge property (**Figure S8b**)
284 between TFC and TFC-TW membranes. This can be explained by the more stable IP
285 reaction interface due to the stabilization effect of TW, which can reduce the formation
286 of defects caused by interfacial instabilities during the IP reaction (**Figure 1b**).[12] In
287 order to further confirm the less defect formation by TW, humic acid (HA) filtration
288 tests were performed. According to Song and Zhou et al.,[26, 63] HA, featuring small size
289 (approximately 1.1-5.4 nm) and soft property, could penetrate the defects instead of
290 transporting through the intact part of polyamide film. The incomplete rejection of HA
291 can be regarded as the evidence for the existence of defects. Generally, TFC-TW

membranes show enhanced HA rejection compared to TFC membranes (**Figure 6c**), indicating that less defects were formed in their polyamide layers. Finally, thanks to the enlarged nanovoids and less defects by TW, TFC-TW membranes show simultaneously increased water permeance and selectivity, particularly at relatively low MPD concentrations (**Figure 6d**).

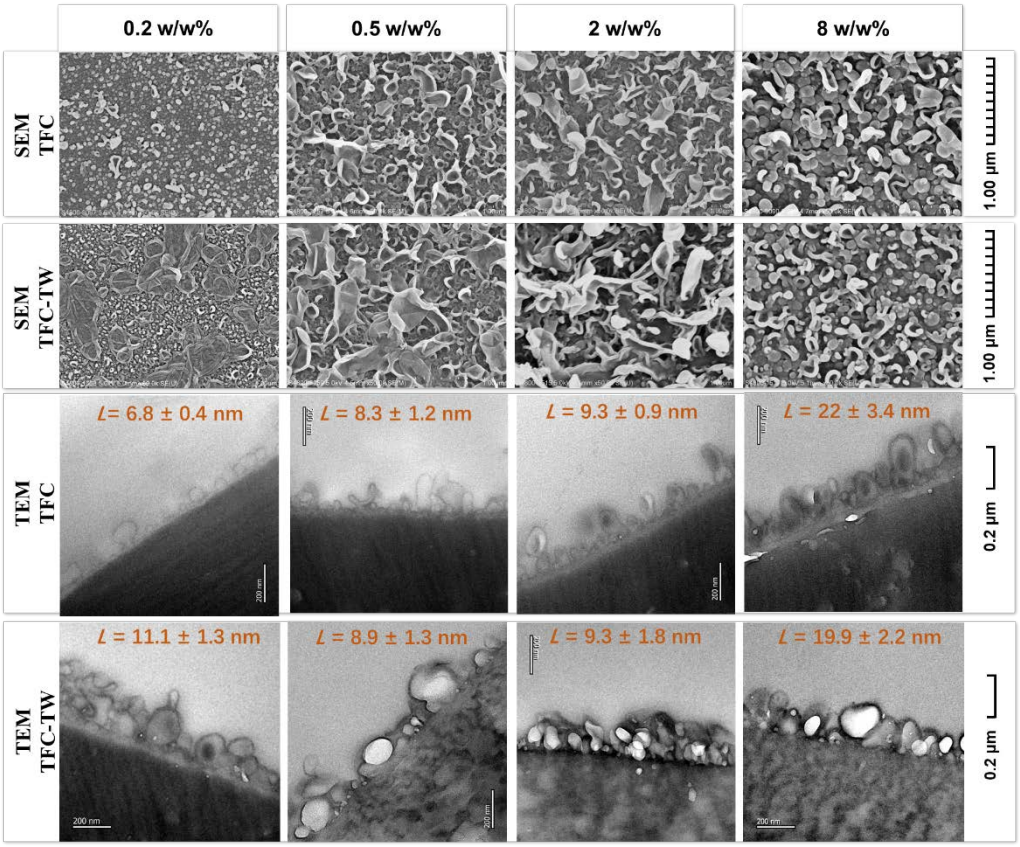

Figure 7. Effects of MPD concentration (at 0.001 w/w% TW) on PA structure (SEM top side view and TEM cross section view). The intrinsic thickness (*L*) of the polyamide film on TEM figures was measured using the software *Image pro plus*.

ENVIRONMENTAL IMPLICATIONS

The current study demonstrated that the surfactant could stabilize the generated nanobubbles at the IP reaction interface to promote the formation of more prominent polyamide nanovoids with reduced defects. This stabilization effect could contribute to the simultaneously enhanced membrane permeance and selectivity. However, when the concentration of surfactant excessed its CMC, micelles formation may negate this stabilization effect and thus deteriorate membrane performance. Future studies need to further optimize the surfactant loading to enhance its stabilization effect for better separation property. In addition, RO membranes often show unsatisfactory removal of viruses and bacteria, possibly due to the defects in the polyamide film.[26, 63] Surfactant-assisted IP may act as a potential strategy for mitigating this penetration thanks to the reduced defects, which calls for more investigations.

We further found that TW addition could reduce membrane fouling propensity–the TFC-TW membrane experienced lower flux decline and less accumulation of HA on its surface compared to the TFC membrane (**Figure 8a** and **b**). The reduced fouling tendency can be attributed to the more prominent nanovoids in TFC-TW, which could potentially regulate the water transport and flux distribution above its polyamide film.[28, 31, 47] Interestingly, TFC shows much sharper flux decline than TFC-TW at the initial stage of fouling test, which can be ascribed to the more defects in its polyamide layer. Since defects can result in hot spots of high localized flux, foulants would preferentially deposit at these regions at the initial stage to accelerate membrane fouling.[58, 64, 65] It is worthwhile to note that the current study only investigated fouling tendency over relatively short filtration duration (96 h). Further studies need to verify the fouling behavior over longer duration. The potential reduction in fouling propensity together with the simultaneously enhanced membrane permeance and selectivity endows the

surfactant-assisted IP strategy with strong potential for future membrane design and optimization.

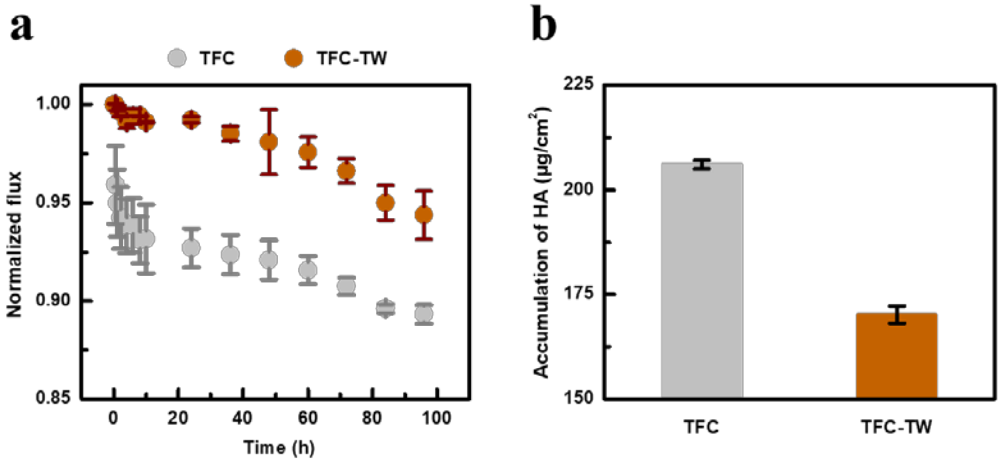

Figure 8. Effects of TW (0.001% w/w) on (a) fouling propensity using HA as a model foulant (100 ppm HA in 2000 ppm NaCl as the feed solution with an initial flux of 17 L m^{-2} h^{-1}, pH at ~6.5) and (b) the accumulation of HA on the membranes after fouling (at MPD concentration of 0.5 w/w%).

ASSOCIATED CONTENT

Supporting Information

The Supporting Information is available free of charge at.

S1, Effects of different surfactants on PA structure, performance, and MPD diffusion; S2, Effects of different surfactants on PA structure at substrate-free IP reaction interface; S3, Surfactant alignment in the IP reaction system; S4, The role of surfactant in bubble formation/stabilization; S5, Effects of TW at different MPD concentrations

AUTHOR INFORMATION

Corresponding Authors

Lu Elfa Peng − *Department of Civil Engineering, The University of Hong Kong, Pokfulam, Hong Kong SAR 999077, P. R., China;* Phone: +852 53964327; Email: elfapeng@connect.hku.hk

Chuyang Y. Tang − *Department of Civil Engineering, The University of Hong Kong, Pokfulam, Hong Kong SAR 999077, P. R., China;* orcid.org/0000-0002-7932-6462; Phone: +852 28591976; Email: tangc@hku.hk

Authors

Qimao Gan − *Department of Civil Engineering, The University of Hong Kong, Pokfulam, Hong Kong SAR 999077, P. R., China;*

Zhe Yang − *Department of Civil Engineering, The University of Hong Kong, Pokfulam, Hong Kong SAR 999077, P. R., China;* orcid.org/0000-0003-0753-3902

Peng-Fei Sun − *Department of Civil Engineering, The University of Hong Kong, Pokfulam, Hong Kong SAR 999077, P. R., China;*

Li Wang − *Department of Civil Engineering, The University of Hong Kong,*

Pokfulam, Hong Kong SAR 999077, P. R., China;

Hao Guo − *Department of Civil Engineering, The University of Hong Kong, Pokfulam, Hong Kong SAR 999077, P. R., China;*

Notes

The authors declare no competing financial interest.

ACKNOWLEDGMENTS

The work was fully supported by a grant from the Research Grants Council of the Hong Kong Special Administration Region, China (SRFS2021-7S04). Lu Elfa Peng is supported by an RGC Postdoctoral Fellowship from the Research Grants Council of the Hong Kong Special Administration Region, China (PDFS2223-7S02). We appreciate the Electron Microscopic Unit (EMU) of the University of Hong Kong for SEM and TEM sample preparation and analysis.

REFERENCES

1. Li, D.; Wang, H. T., Recent developments in reverse osmosis desalination membranes. *J. Mater. Chem.* **2010,** *20*, (22), 4551-4566.
2. Elimelech, M.; Phillip, W. A., The future of seawater desalination: energy, technology, and the environment. *Science* **2011,** *333*, (6043), 712-7.
3. Tang, C. Y.; Yang, Z.; Guo, H.; Wen, J. J.; Nghiem, L. D.; Cornelissen, E., Potable Water Reuse through Advanced Membrane Technology. *Environ. Sci. Technol.* **2018,** *52*, (18), 10215-10223.
4. Guo, H.; Li, X.; Yang, W.; Yao, Z.; Mei, Y.; Peng, L. E.; Yang, Z.; Shao, S.; Tang, C. Y., Nanofiltration for drinking water treatment: a review. *Front Chem Sci Eng* **2022,** *16*, (5), 681-698.
5. Jimenez-Solomon, M. F.; Song, Q. L.; Jelfs, K. E.; Munoz-Ibanez, M.; Livingston, A. G., Polymer nanofilms with enhanced microporosity by interfacial polymerization. *Nat. Mater.* **2016,** *15*, (7), 760.
6. Park, H. B.; Kamcev, J.; Robeson, L. M.; Elimelech, M.; Freeman, B. D., Maximizing the right stuff: The trade-off between membrane permeability and selectivity. *Science* **2017,** *356*, (6343), eaab0530.
7. Elimelech, M.; Zhu, X. H.; Childress, A. E.; Hong, S. K., Role of membrane surface morphology in colloidal fouling of cellulose acetate and composite aromatic polyamide reverse osmosis membranes. *J. Membr. Sci.* **1997,** *127*, (1), 101-109.
8. Yan, H.; Miao, X.; Xu, J.; Pan, G.; Zhang, Y.; Shi, Y.; Guo, M.; Liu, Y., The porous structure of the fully-aromatic polyamide film in reverse osmosis membranes. *J. Membr. Sci.* **2015,** *475*, 504-510.
9. Kong, C.; Kanezashi, M.; Yamomoto, T.; Shintani, T.; Tsuru, T., Controlled synthesis of high performance polyamide membrane with thin dense layer for water desalination. *J. Membr. Sci.* **2010,** *362*, (1-2), 76-80.
10. Guo, H.; Dai, R.; Xie, M.; Peng, L. E.; Yao, Z.; Yang, Z.; Nghiem, L. D.; Snyder, S. A.; Wang, Z.; Tang, C. Y., Tweak in Puzzle: Tailoring Membrane Chemistry and Structure toward Targeted Removal of Organic Micropollutants for Water Reuse. *Environ. Sci. Technol. Lett.* **2022,** *9*, (4), 247-257.
11. Yang, Z.; Guo, H.; Tang, C. Y. Y., The upper bound of thin-film composite (TFC) polyamide membranes for desalination. *J. Membr. Sci.* **2019,** *590*, 117297.
12. Freger, V.; Ramon, G. Z., Polyamide desalination membranes: Formation, structure, and properties. *Prog. Polym. Sci.* **2021,** *122*, 101451.
13. Lu, X.; Elimelech, M., Fabrication of desalination membranes by interfacial polymerization: history, current efforts, and future directions. *Chem. Soc. Rev.* **2021,** *50*, (11),

406 6290-6307.
407 14. Cui, Y.; Liu, X.-Y.; Chung, T.-S., Ultrathin Polyamide Membranes Fabricated from
408 Free-Standing Interfacial Polymerization: Synthesis, Modifications, and Post-treatment. *Ind.*
409 *Eng. Chem. Res.* **2017,** *56*, (2), 513-523.
410 15. Lau, W. J.; Ismail, A. F.; Misdan, N.; Kassim, M. A., A recent progress in thin film
411 composite membrane: A review. *Desalination* **2012,** *287*, 190-199.
412 16. Klaysom, C.; Hermans, S.; Gahlaut, A.; Van Craenenbroeck, S.; Vankelecom, I. F. J.,
413 Polyamide/Polyacrylonitrile (PA/PAN) thin film composite osmosis membranes: Film
414 optimization, characterization and performance evaluation. *J. Membr. Sci.* **2013,** *445*, 25-33.
415 17. Cui, Y.; Liu, X.-Y.; Chung, T.-S., Enhanced osmotic energy generation from salinity
416 gradients by modifying thin film composite membranes. *Chem. Eng. J.* **2014,** *242*, 195-203.
417 18. Mansourpanah, Y.; Alizadeh, K.; Madaeni, S. S.; Rahimpour, A.; Soltani Afarani, H.,
418 Using different surfactants for changing the properties of poly(piperazineamide) TFC
419 nanofiltration membranes. *Desalination* **2011,** *271*, (1-3), 169-177.
420 19. Mansourpanah, Y.; Madaeni, S. S.; Rahimpour, A., Fabrication and development of
421 interfacial polymerized thin-film composite nanofiltration membrane using different
422 surfactants in organic phase; study of morphology and performance. *J. Membr. Sci.* **2009,** *343*,
423 (1-2), 219-228.
424 20. Liang, Y.; Zhu, Y.; Liu, C.; Lee, K. R.; Hung, W. S.; Wang, Z.; Li, Y.; Elimelech, M.;
425 Jin, J.; Lin, S., Polyamide nanofiltration membrane with highly uniform sub-nanometre pores
426 for sub-1 A precision separation. *Nat Commun* **2020,** *11*, (1), 2015.
427 21. Sarkar, P.; Modak, S.; Karan, S., Ultraselective and Highly Permeable Polyamide
428 Nanofilms for Ionic and Molecular Nanofiltration. *Adv. Funct. Mater.* **2021,** *31*, (3), 2007054.
429 22. Al-Jeshi, S.; Neville, A., An investigation into the relationship between flux and
430 roughness on RO membranes using scanning probe microscopy. *Desalination* **2006,** *189*, (1-3),
431 221-228.
432 23. Hirose, M.; Minamizaki, Y.; Kamiyama, Y., The relationship between polymer
433 molecular structure of RO membrane skin layers and their RO performances. *J. Membr. Sci.*
434 **1997,** *123*, (2), 151-156.
435 24. Lin, L.; Lopez, R.; Ramon, G. Z.; Coronell, O., Investigating the void structure of the
436 polyamide active layers of thin-film composite membranes. *J. Membr. Sci.* **2016,** *497*, 365-376.
437 25. Pacheco, F.; Sougrat, R.; Reinhard, M.; Leckie, J. O.; Pinnau, I., 3D visualization of
438 the internal nanostructure of polyamide thin films in RO membranes. *J. Membr. Sci.* **2016,** *501*,
439 33-44.
440 26. Song, X.; Gan, B.; Qi, S.; Guo, H.; Tang, C. Y.; Zhou, Y.; Gao, C., Intrinsic Nanoscale
441 Structure of Thin Film Composite Polyamide Membranes: Connectivity, Defects, and

Structure-Property Correlation. *Environ. Sci. Technol.* **2020,** *54*, (6), 3559-3569.
27. Peng, L. E.; Gan, Q. M.; Yang, Z.; Wang, L.; Sun, P. F.; Guo, H.; Park, H. D.; Tang, C. Y., Deciphering the Role of Amine Concentration on Polyamide Formation toward Enhanced RO Performance. *Acs ES&T Engineering* **2022,** *2*, (5), 903-912.
28. Wong, M. C. Y.; Lin, L.; Coronell, O.; Hoek, E. M. V.; Ramon, G. Z., Impact of liquid-filled voids within the active layer on transport through thin-film composite membranes. *J. Membr. Sci.* **2016,** *500*, 124-135.
29. Yang, Z.; Sun, P. F.; Li, X.; Gan, B.; Wang, L.; Song, X.; Park, H. D.; Tang, C. Y., A Critical Review on Thin-Film Nanocomposite Membranes with Interlayered Structure: Mechanisms, Recent Developments, and Environmental Applications. *Environ. Sci. Technol.* **2020,** *54*, (24), 15563-15583.
30. Peng, L. E.; Yang, Z.; Long, L.; Zhou, S.; Guo, H.; Tang, C. Y., A critical review on porous substrates of TFC polyamide membranes: Mechanisms, membrane performances, and future perspectives. *J. Membr. Sci.* **2022,** *641*, 119871.
31. Shao, S.; Zeng, F.; Long, L.; Zhu, X.; Peng, L. E.; Wang, F.; Yang, Z.; Tang, C. Y., Nanofiltration Membranes with Crumpled Polyamide Films: A Critical Review on Mechanisms, Performances, and Environmental Applications. *Environ. Sci. Technol.* **2022,** *56*, (18), 12811-12827.
32. Ma, X.-H.; Yao, Z.-K.; Yang, Z.; Guo, H.; Xu, Z.-L.; Tang, C. Y.; Elimelech, M., Nanofoaming of Polyamide Desalination Membranes To Tune Permeability and Selectivity. *Environ. Sci. Technol. Lett.* **2018,** *5*, (2), 123-130.
33. Ma, X.; Yang, Z.; Yao, Z.; Guo, H.; Xu, Z.; Tang, C. Y., Tuning roughness features of thin film composite polyamide membranes for simultaneously enhanced permeability, selectivity and anti-fouling performance. *J. Colloid Interface Sci.* **2019,** *540*, 382-388.
34. Song, X.; Gan, B.; Yang, Z.; Tang, C. Y.; Gao, C., Confined nanobubbles shape the surface roughness structures of thin film composite polyamide desalination membranes. *J. Membr. Sci.* **2019,** *582*, 342-349.
35. Peng, L. E.; Yao, Z.; Liu, X.; Deng, B.; Guo, H.; Tang, C. Y., Tailoring Polyamide Rejection Layer with Aqueous Carbonate Chemistry for Enhanced Membrane Separation: Mechanistic Insights, Chemistry-Structure-Property Relationship, and Environmental Implications. *Environ. Sci. Technol.* **2019,** *53*, (16), 9764-9770.
36. Peng, L. E.; Yao, Z.; Yang, Z.; Guo, H.; Tang, C. Y., Dissecting the Role of Substrate on the Morphology and Separation Properties of Thin Film Composite Polyamide Membranes: Seeing Is Believing. *Environ. Sci. Technol.* **2020,** *54*, (11), 6978-6986.
37. Peng, L. E.; Jiang, Y.; Wen, L.; Guo, H.; Yang, Z.; Tang, C. Y., Does interfacial vaporization of organic solvent affect the structure and separation properties of polyamide RO

membranes? *J. Membr. Sci.* **2021,** *625*, 119173.
38. Zhang, X.; Chan, D. Y.; Wang, D.; Maeda, N., Stability of interfacial nanobubbles. *Langmuir* **2013,** *29*, (4), 1017-23.
39. Alheshibri, M.; Qian, J.; Jehannin, M.; Craig, V. S., A History of Nanobubbles. *Langmuir* **2016,** *32*, (43), 11086-11100.
40. An, H.; Liu, G.; Atkin, R.; Craig, V. S., Surface Nanobubbles in Nonaqueous Media: Looking for Nanobubbles in DMSO, Formamide, Propylene Carbonate, Ethylammonium Nitrate, and Propylammonium Nitrate. *ACS Nano* **2015,** *9*, (7), 7596-607.
41. Gor, G. Y.; Kuchma, A. E., Dynamics of gas bubble growth in a supersaturated solution with Sievert's solubility law. *J. Chem. Phys.* **2009,** *131*, (3), 034507.
42. Xu, Q.; Nakajima, M.; Ichikawa, S.; Nakamura, N.; Roy, P.; Okadome, H.; Shiina, T., Effects of surfactant and electrolyte concentrations on bubble formation and stabilization. *J. Colloid Interface Sci.* **2009,** *332*, (1), 208-14.
43. Wu, Y.; Fang, S.; Zhang, K.; Zhao, M.; Jiao, B.; Dai, C., Stability Mechanism of Nitrogen Foam in Porous Media with Silica Nanoparticles Modified by Cationic Surfactants. *Langmuir* **2018,** *34*, (27), 8015-8023.
44. Zhang, X. H.; Maeda, N.; Craig, V. S., Physical properties of nanobubbles on hydrophobic surfaces in water and aqueous solutions. *Langmuir* **2006,** *22*, (11), 5025-35.
45. Oeffinger, B. E.; Wheatley, M. A., Development and characterization of a nano-scale contrast agent. *Ultrasonics* **2004,** *42*, (1-9), 343-7.
46. Bae, Y.; Kang, S.; Kim, B. H.; Lim, K.; Jeon, S.; Shim, S.; Lee, W. C.; Park, J., Nanobubble Dynamics in Aqueous Surfactant Solutions Studied by Liquid-Phase Transmission Electron Microscopy. *Engineering* **2021,** *7*, (5), 630-635.
47. Gan, Q.; Peng, L. E.; Guo, H.; Yang, Z.; Tang, C. Y., Cosolvent-Assisted Interfacial Polymerization toward Regulating the Morphology and Performance of Polyamide Reverse Osmosis Membranes: Increased m-Phenylenediamine Solubility or Enhanced Interfacial Vaporization? *Environ. Sci. Technol.* **2022,** *56*, (14), 10308-10316.
48. Karan, S.; Jiang, Z. W.; Livingston, A. G., Sub-10 nm polyamide nanofilms with ultrafast solvent transport for molecular separation. *Science* **2015,** *348*, (6241), 1347-1351.
49. Jiang, Z.; Karan, S.; Livingston, A. G., Water Transport through Ultrathin Polyamide Nanofilms Used for Reverse Osmosis. *Adv. Mater.* **2018,** *30*, (15), 1705973.
50. Yang, Z.; Wang, F.; Guo, H.; Peng, L. E.; Ma, X. H.; Song, X. X.; Wang, Z.; Tang, C. Y., Mechanistic Insights into the Role of Polydopamine Interlayer toward Improved Separation Performance of Polyamide Nanofiltration Membranes. *Environ. Sci. Technol.* **2020,** *54*, (18), 11611-11621.
51. Long, L.; Wu, C.; Yang, Z.; Tang, C. Y., Carbon Nanotube Interlayer Enhances Water

514 Permeance and Antifouling Performance of Nanofiltration Membranes: Mechanisms and
515 Experimental Evidence. *Environ. Sci. Technol.* **2022,** *56,* (4), 2656-2664.
516 52. Wang, L.; Cao, T.; Dykstra, J. E.; Porada, S.; Biesheuvel, P. M.; Elimelech, M., Salt
517 and Water Transport in Reverse Osmosis Membranes: Beyond the Solution-Diffusion Model.
518 *Environ. Sci. Technol.* **2021,** *55,* (24), 16665-16675.
519 53. Ritt, C. L.; Stassin, T.; Davenport, D. M.; DuChanois, R. M.; Nulens, I.; Yang, Z.; Ben-
520 Zvi, A.; Segev-Mark, N.; Elimelech, M.; Tang, C. Y.; Ramon, G. Z.; Vankelecom, I. F. J.;
521 Verbeke, R., The open membrane database: Synthesis–structure–performance relationships of
522 reverse osmosis membranes. *J. Membr. Sci.* **2022,** *641*, 119927.
523 54. Wu, J.; West, L. J.; Stewart, D. I., Effect of humic substances on Cu(II) solubility in
524 kaolin-sand soil. *J. Hazard. Mater.* **2002,** *94,* (3), 223-38.
525 55. Klučáková, M.; Kalina, M., Composition, particle size, charge, and colloidal stability
526 of pH-fractionated humic acids. *Journal of Soils and Sediments* **2015,** *15,* (9), 1900-1908.
527 56. Hong, S. K.; Elimelech, M., Chemical and physical aspects of natural organic matter
528 (NOM) fouling of nanofiltration membranes. *J. Membr. Sci.* **1997,** *132,* (2), 159-181.
529 57. Seidel, A.; Elimelech, M., Coupling between chemical and physical interactions in
530 natural organic matter (NOM) fouling of nanofiltration membranes: implications for fouling
531 control. *J. Membr. Sci.* **2002,** *203,* (1-2), 245-255.
532 58. Tang, C. Y. Y.; Kwon, Y. N.; Leckie, J. O., Characterization of humic acid fouled
533 reverse osmosis and nanofiltration membranes by transmission electron microscopy and
534 streaming potential measurements. *Environ. Sci. Technol.* **2007,** *41,* (3), 942-949.
535 59. Shinshi, M.; Sugihara, T.; Osakai, T.; Goto, M., Electrochemical extraction of proteins
536 by reverse micelle formation. *Langmuir* **2006,** *22,* (13), 5937-44.
537 60. Chowdhury, M.; Kataky, R., Emulsification at the Liquid/Liquid Interface: Effects of
538 Potential, Electrolytes and Surfactants. *Chemphyschem* **2016,** *17,* (1), 105-11.
539 61. Xu, J.; Yan, H.; Zhang, Y.; Pan, G.; Liu, Y., The morphology of fully-aromatic
540 polyamide separation layer and its relationship with separation performance of TFC membranes.
541 *J. Membr. Sci.* **2017,** *541*, 174-188.
542 62. Park, S.-J.; Kwon, S. J.; Kwon, H.-E.; Shin, M. G.; Park, S.-H.; Park, H.; Park, Y.-I.;
543 Nam, S.-E.; Lee, J.-H., Aromatic solvent-assisted interfacial polymerization to prepare high
544 performance thin film composite reverse osmosis membranes based on hydrophilic supports.
545 *Polymer* **2018,** *144*, 159-167.
546 63. Zhou, S.; Long, L.; Yang, Z.; So, S. L.; Gan, B.; Guo, H.; Feng, S. P.; Tang, C. Y.,
547 Unveiling the Growth of Polyamide Nanofilms at Water/Organic Free Interfaces: Toward
548 Enhanced Water/Salt Selectivity. *Environ. Sci. Technol.* **2022,** *56*, (14), 10279-10288.
549 64. Ramon, G. Z.; Wong, M. C. Y.; Hoek, E. M. V., Transport through composite

membrane, part 1: Is there an optimal support membrane? *J. Membr. Sci.* **2012,** *415-416*, 298-305.

65. Liu, J.; Tang, Z.; Yang, H.; Li, X.; Yu, X.; Wang, Z.; Huang, T.; Tang, C. Y., Dissecting the role of membrane defects with low-energy barrier on fouling development through A collision Attachment-Monte Carlo approach. *J. Membr. Sci.* **2022,** *663*, 120981.